

Gangliosides' Inhibitory Effects on NAD Glycohydrolase: Estimating the Solvation Effect in the Physiological Environment

Kaori Ueno-Noto,[1] Miki Hara-Yokoyama,[2] and Keiko Takano*[1]

[1]Graduate School of Humanities and Sciences and the Glycoscience Institute, Ochanomizu University, 2-1-1 Otsuka, Bunkyo-ku, Tokyo 112-8610

[2]Section of Biochemistry, Department of Hard Tissue Engineering, Division of Bio-Matrix, Graduate School, Tokyo Medical and Dental University, 1-5-45 Yushima, Bunkyo-ku, Tokyo 113-8549

Received July 30, 2007; E-mail: takano.keiko@ocha.ac.jp

The solvation effect was considered in order to interpret the causative factors of the differences in gangliosides' inhibitory effects on CD38, an enzyme nicotinamide adenine dinucleotide (NAD) glycohydrolase, as well as the mechanisms by which the gangliosides recognize CD38, in the biological system. We applied the two-layered our own N-layered integrated molecular orbital and molecular mechanics (ONIOM) method as well as the supermolecule method to a large solvated system. For comparison, the conductor-like screening model (COSMO) was applied to the same system. The orbital energy of the highest occupied molecular orbital (HOMO) was correlated with the strength of the gangliosides' inhibitory effect in both the supermolecule and ONIOM methods; this agrees with our previous results in the gas phase. Solvation only slightly affected both the structures of tandem sialic acid residues themselves and the energy profiles of HOMOs of gangliosides. These results support the previously proposed recognition mechanism, in which CD38 is likely to recognize the two phosphate groups in the substrate, NAD, as well as the two carboxyl groups in gangliosides' tandem sialic acid residues.

CD38 has the enzymatic activity of nicotinamide adenine dinucleotide glycohydrolase (NADase) in its extracellular domain. Gangliosides are glycosphingolipids having one or more sialic acids. A series of gangliosides has been reported to inhibit the enzyme activity of CD38 as an NAD glycohydrolase. In addition, b-series of gangliosides with tandem sialic acid residues in the sugar chain greatly inhibited NADase.[1–4] Figure 1a shows a simplified illustration of the b-series gangliosides and their inhibitory strength. We have attempted to clarify the causative factors of the differences in inhibitory effects among gangliosides and the recognition mechanisms of the enzyme based on the competitive reaction model between NAD (Chart 1) and gangliosides. Two carboxyl groups of the tandem sialic acid residues in gangliosides might mimic the diphosphate moiety of NAD as a substrate, thereby inhibiting NADase activity. In our previous paper, we reported that the dipole moments and orbital energies of HOMOs obtained by quantum mechanical calculation of gangliosides and the substrate were well correlated with their inhibitory effects.[5] By analyzing the gangliosides' electronic structures, we also found that CD38 was likely to recognize the two carboxyl groups in tandem sialic acid residues of gangliosides, as well as the phosphate groups in the substrate. This type of recognition is consistent with the crystal structure of a homologue protein of CD38, ADP-ribosyl cyclase, with substrate analogues reported by Love et al.[6] They showed that the Glu179 residue containing two carboxyl groups plays an important role in this enzyme activity and is covalently bonded to the substrate analogue.

The solvation effect is an important factor when we interpret the substrate recognition mechanisms in the biological system. The enzyme reactions in biological systems usually contain large molecules in a massive number of solvent molecules. Accurate ab initio calculations of such biological systems are still very challenging despite the prominent computational progress that has been made lately. Quite a few papers concerning solvation models have appeared, which should be ultimately used for reaction mechanisms in biological systems. Such models include, for example, the Onsager model of self-consistent reaction field (SCRF)[7,8] and the polarizable dielectric continuum model (PCM). The PCM models, in which a cavity is created via a series of overlapping spheres, was initially devised by Tomasi and his co-workers.[9,10] The conductor-like screening model (COSMO) developed by Klamt and Schuumann is one of the PCM models and has been used to explore the solvated system.[11] Several other PCM methods, such as the static isodensity surface polarized continuum model (IPCM) and self-consistent isodensity PCM model, have also been reported.[12]

The advantage of including the explicit water molecules has been pointed out. In the supermolecule method, solute and solvent are treated as a supermolecule. In this context, this method has already been applied to the study of solvent effects on a nucleic acid by explicitly considering a few water molecules.[13,14] We applied the supermolecule method to the systems studied in this work.

In the present study, we examined the mechanism by which gangliosides inhibit NADase in the biological system. Gangliosides contain large numbers of atoms, which made it difficult to perform most of the methods described above because of the computational limitation. Thus, the solvation effect was considered by the use of quantum mechanics/molecular mechanics (QM/MM) methods. ONIOM[15–17] is a QM/MM method that has been applied to the study of complex organic reac-

Published on the web September 11, 2008; doi:10.1246/bcsj.81.1062

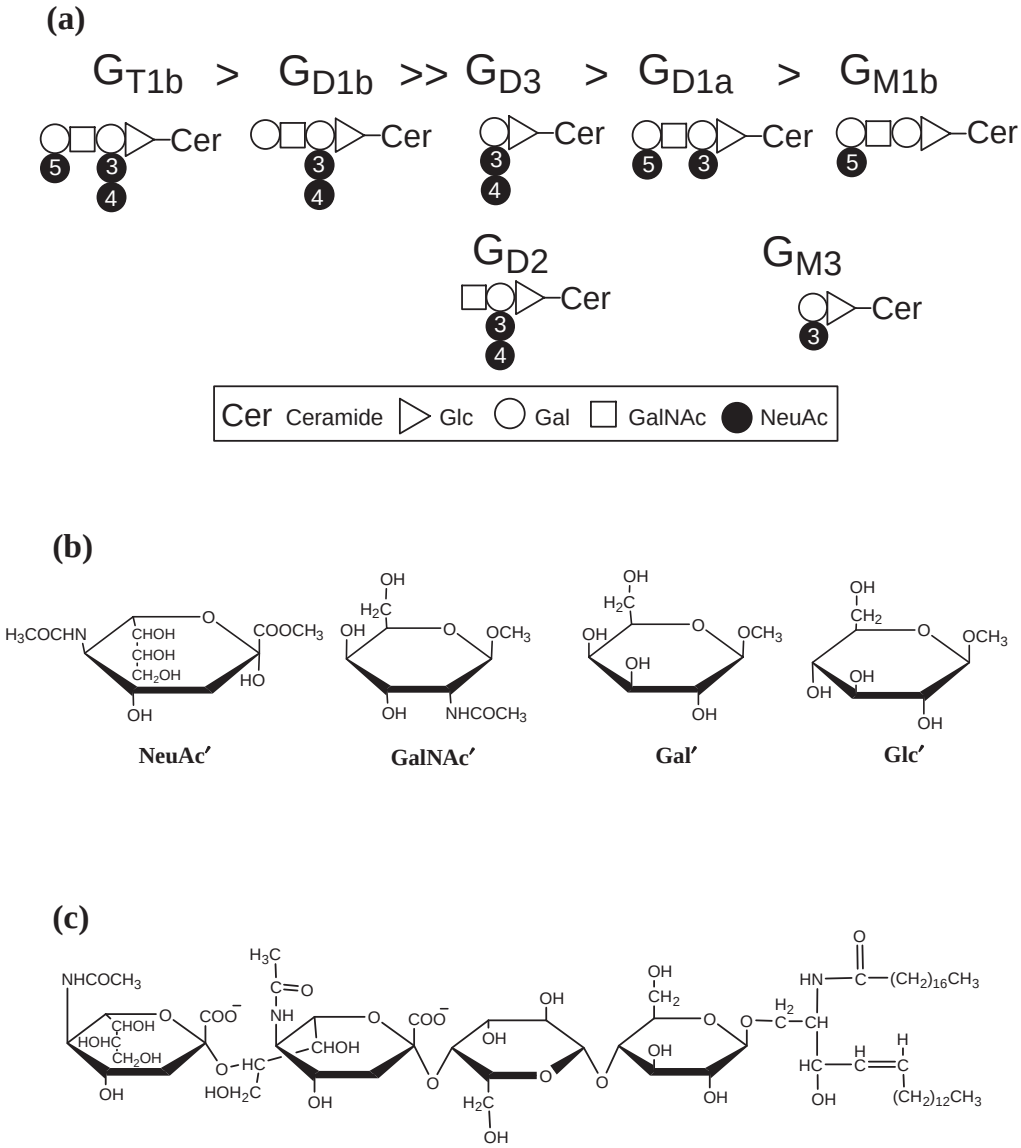

Figure 1. (a) Topological models of the b-series of gangliosides having an inhibitory effect against NADase, CD38. In addition to the gangliosides studied experimentally, G_{D2} and G_{M3} were also considered for comparison. The numerical order of the sialic acids is depicted as the distance from the ceramide part. (b) Chemical structures of the studied methyl derivatives of component monosaccharides, α-*N*-acetylneuraminic acid (NeuAc′), β-*N*-acetylgalactosamine (GalNAc′), β-D-galactose (Gal′), and β-D-glucose (Glc′). (c) Primary and chemical structures of ganglioside G_{D3}.

tion systems, such as organometallic reactions, and has recently been applied to models of enzymatic reactions.[18,19] ONIOM allows us to use a combination of expensive and inexpensive theories to make highly accurate computations possible on large molecules. This method can also divide the system into layers using MO and/or MM calculations with different levels of accuracy. It has also been applied to relatively small solvated systems such as micro-solvated clusters[20] and to relatively large systems such as ethyl chlorophyllide-*a* and Cu/Zn superoxide dismutase.[21,22] Regarding solvation for biomolecules, Zhang et al. studied the solvation system of a nucleic acid with different levels of the ONIOM method.[23] They considered seven water molecules as the first hydration shell and showed that ONIOM is an effective tool for studying solvated systems. In this study, we applied the ONIOM method to our system including large biomolecules of 84 to 147 atoms.

Two of the aims of this study are to model gangliosides' inhibitory effect on the NAD glycohydrolase of CD38 in the physiological environment and to illustrate the causative factor of the recognition mechanisms more clearly. A third goal is to analyze the solvation effect on our systems by applying the supermolecule and ONIOM methods to a solute–solvent system including large solute molecules.

Computational Methods

Monosaccharides, such as β-D-glucose, β-D-galactose, β-*N*-acetylgalactosamine, and α-*N*-acetylneuraminic acid, are the components of gangliosides. First, we studied the methyl de-

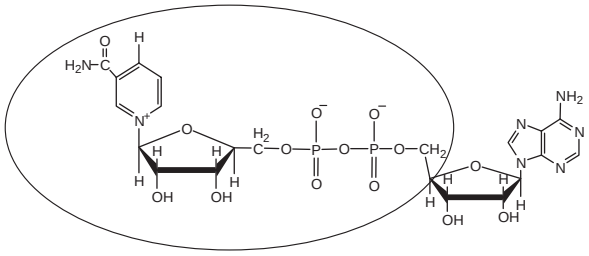

NAD

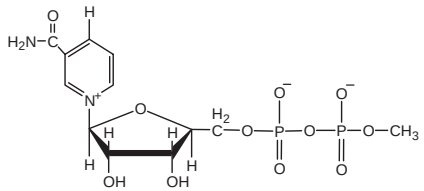

Model compound (NAD′)

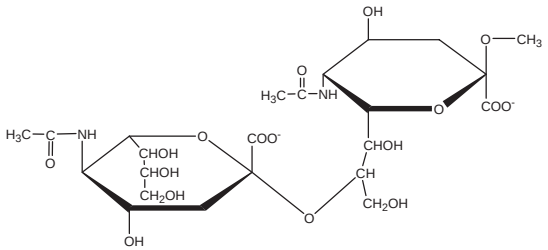

Dimeric sialic acid $(NeuAc)_2$

Chart 1.

rivatives of α-*N*-acetylneuraminic acid (NeuAc′), β-*N*-acetylgalactosamine (GalNAc′), β-D-galactose (Gal′), and β-D-glucose (Glc′) (Figure 1b). We then studied the analogue of the enzyme substrate, a model compound of nicotinamide adenine dinucleotide (NAD), whose adenosine group was substituted to the methyl group. It is designated as NAD′ (Chart 1). In addition, dimeric sialic acid $(NeuAc)_2$ was taken as a model of tandem sialic acid residues of gangliosides, which is thought to be responsible for this enzyme reaction. Four gangliosides were also studied: G_{M3}, G_{D2}, G_{M1b}, and G_{D3}. The chemical structure of G_{D3} is depicted in Figure 1c. We concentrated on the oligosaccharide parts (the "head group"), since they are considered to be extruded from the biological membrane and to interact with the enzyme.

The procedure for making input geometries for ONIOM calculations is depicted in Figure 2. First, the geometry of the isolated solute molecule, which corresponds to the one in the gas phase, was optimized by the PM3 method. Next, water molecules were generated arbitrarily in a three-dimensional box of an appropriate size for the solutes. Then, the solute molecule having the PM3-optimized geometry was placed at the center of the box and was replaced with several water molecules there. This procedure was done with the aid of the TINKER program, ver. 3.9.[24] The extra water molecules outside of the first hydration sphere were cut off manually by tracing the space-filling model of the solute. For the system thus obtained, two-layered ONIOM calculations were applied. The solute molecules studied in this work and the numbers of solvent water molecules are listed in Table 1. The solute and the solvent were, respectively, the first and second layers of the model. The geometries were optimized with the ONIOM(PM3:UFF) and ONIOM(RHF/3-21G:PM3) methods. The ONIOM energy for a two-layer system was calculated by eq 1.

$$E(\text{High, Real}) = E(\text{ONIOM}) = E(\text{Low, Model}) + \text{size} + \text{level} = E(\text{Low, Real}) + E(\text{High, Model}) - E(\text{Low, Model}) \quad (1)$$

The full molecular geometry including all atoms is referred to as the "Real" geometry, and it is treated using a "Low" level of theory. A subset of the atoms, called the "Model" geometry, is treated using both the "Low" and "High" levels of theory.[15] The full system, containing a solute and solvent molecules as a "Real" system, was treated using MM calculations with UFF (universal force field) parameters[25] as a "Low" level of theory. The solute, which is a subset of the atoms, as a "Model" system was managed by MM with UFF parameters as the "Low" level and PM3 molecular orbital (MO) calculations as a "High" level of theory. This combination of theory levels is referred to as ONIOM(PM3:UFF). We applied a better combination of the ONIOM method to this system: RHF/3-21G and PM3 for the "High" and "Low" levels, respectively, which is abbreviated as ONIOM(RHF/3-21G:PM3). The geometry of the whole system consisting of the solute and solvent waters was optimized as a supermolecule by the PM3 method. Then, single-point energy calculations of the whole system were carried out using a much larger basis set RHF/6-31++G(d,p) at the ONIOM(PM3:UFF), ONIOM(RHF/3-21G:PM3), and Supermolecule(PM3) optimized geometries.

COSMO, a dielectric model calculation method[11] implemented in MOPAC2000, was performed for comparison. The dielectric constant of water (78.4) was used to translate the physiological system.

To estimate how much the solvent effect on the head group induces structural change and consequent energy change, we calculated the energy difference between the PM3 optimized geometry of each ganglioside as an isolated system and the geometry of each ganglioside as a solute in the hydrated system optimized by ONIOM(PM3:UFF).

All the ONIOM, ab initio, and PM3 calculations were carried out using the Gaussian 03 program.[26] The computers used in this study were Linux PC cluster machines at Ochanomizu University. Computer facilities at the Research Center for Computational Science, Okazaki Research Facilities, National Institutes of Natural Sciences, Japan, were also used.

Results and Discussion

Solvation Effect on Methyl Derivatives of Monosaccharides. The geometric parameters and orbital energies of the methyl derivatives of monosaccharides Glc′, Gal′, GalNAc′, and NeuAc′ were investigated to compare the various computational methods of examining the solvation effect. For comparison, $(NeuAc)_2$ and the model compound NAD′ were also studied.

The geometric parameters of the glycoside bond for the methyl derivatives of the monosaccharides are listed in Table 2. The calculation methods differed only slightly in calculated bond lengths $r1$ and $r2$ and bond angle θ. In contrast,

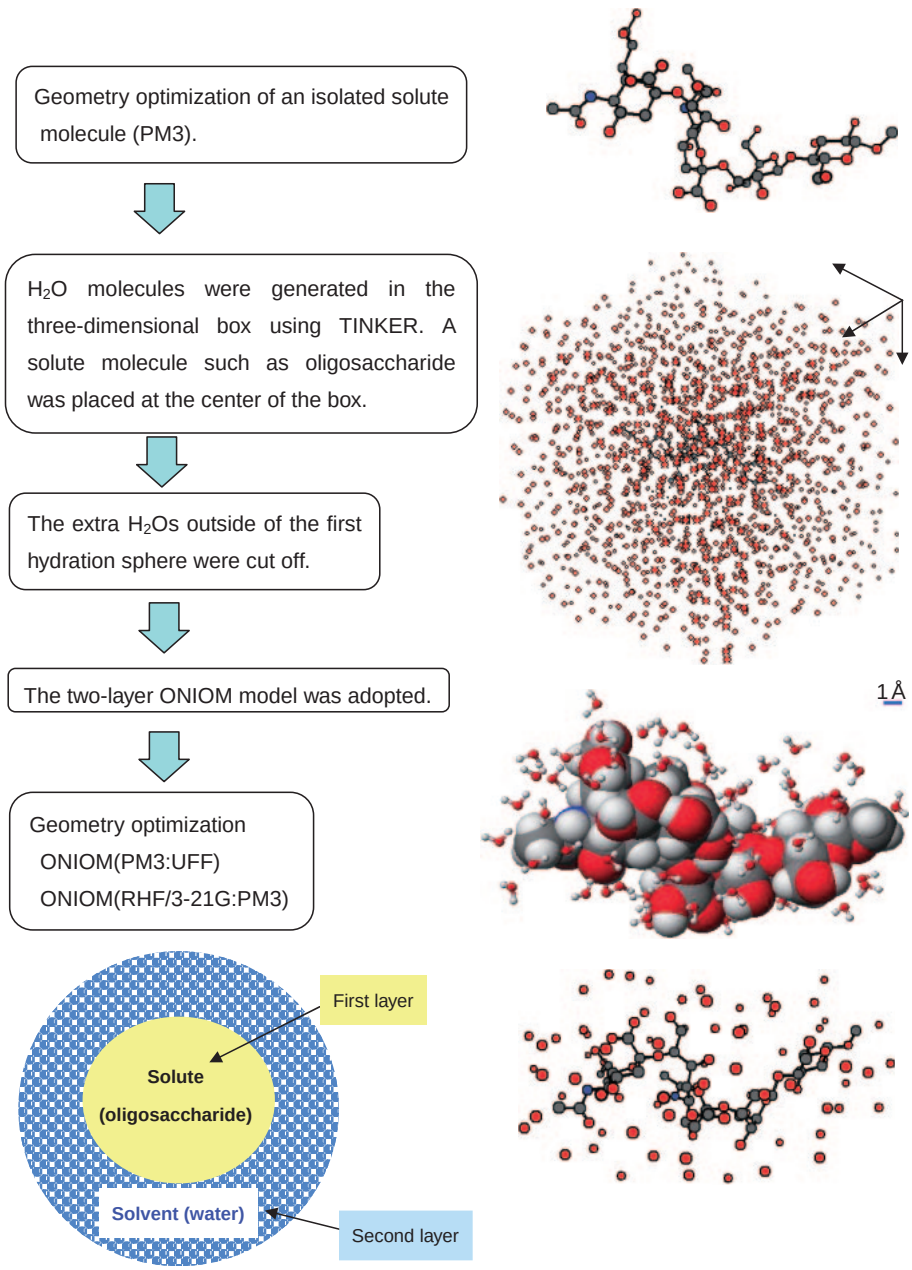

Figure 2. ONIOM calculation procedure.

Table 1. Number of Water Molecules in the First Hydration Cell

	Gangliosides[a)]				Monosaccharides[b)]				Dimeric sialic acid $(NeuAc)_2$	NAD′
	G_{M3}	G_{D2}	G_{D3}	G_{M1b}	Gal′	Glc′	GalNAc′	NeuAc′		
Number of H_2O molecules	38	57	67	72	31	35	26	31	44	31

a) Head group of gangliosides was used for calculations. b) Methyl derivatives of monosaccharides were adopted as models for the components of the studied gangliosides.

the dihedral angle ϕ differed significantly among the methods.

The bond lengths $r1$ and $r2$ were almost the same for all the calculations with and without solvent. As for the angle θ of the glycoside bond, the θ value of NeuAc′ was slightly affected by the solvent. The change in θ was less than 1.2 degrees. In contrast with $r1$, $r2$, and θ, dihedral angle ϕ was greatly affected by solvation, and the method dependency was fairly large. The differences in dihedral angles, $\Delta_{dihedral}$, between the solvated system treated by the ONIOM(PM3:UFF) and Supermolecule(PM3) methods and isolated systems were estimated as

Table 2. Geometric Parameters of Glycoside Bond and O–CH_3 Bond of Monosaccharides Calculated with Various Methods

		Glc′	Δ[b)]	Gal′	Δ[b)]	GalNAc′	Δ[b)]	NeuAc′	Δ[b)]
ONIOM(PM3:UFF)	$r1$/Å[a)]	1.41	0.00	1.41	0.00	1.41	0.00	1.41	0.00
	$r2$/Å[a)]	1.41	0.00	1.41	0.00	1.41	0.00	1.41	0.00
	θ/°	115.3	0.0	115.2	0.0	115.1	−0.1	116.7	0.2
	ϕ/°	−99.3	−5.3	−93.3	−7.8	−92.7	−2.3	90.3	0.5
ONIOM(RHF/3-21G:PM3)	$r1$/Å[a)]	1.40	−0.01	1.40	−0.01	1.40	−0.01	1.41	0.00
	$r2$/Å[a)]	1.45	0.04	1.45	0.04	1.45	0.04	1.45	0.04
	θ/°	116.2	0.9	115.9	0.7	116.4	1.2	117.4	0.9
	ϕ/°	−61.4	32.6	−59.1	32.4	−55.0	35.5	59.1	30.7
Supermolecule(PM3)	$r1$/Å[a)]	1.41	0.00	1.41	0.00	1.41	0.00	1.41	0.00
	$r2$/Å[a)]	1.41	0.00	1.41	0.00	1.41	0.00	1.41	0.00
	θ/°	115.2	−0.1	115.1	−0.1	115.8	0.6	117.7	1.2
	ϕ/°	−94.4	−0.4	−98.5	−7.0	−96.0	−5.0	84.9	−4.9
COSMO(PM3)	$r1$/Å[a)]	1.42	0.01	1.42	0.01	1.41	0.00	1.42	0.01
	$r2$/Å[a)]	1.41	0.00	1.41	0.00	1.41	0.00	1.41	0.00
	θ/°	114.7	−0.6	114.5	−0.7	115.4	0.2	117.5	1.0
	ϕ/°	−157.2	−63.2	−153.9	−62.4	−129.6	−39.1	74.0	−15.8
Isolated system (PM3)	$r1$/Å[a)]	1.41	—	1.41	—	1.41	—	1.41	—
	$r2$/Å[a)]	1.41	—	1.41	—	1.41	—	1.41	—
	θ/°	115.3	—	115.2	—	115.2	—	116.5	—
	ϕ/°	−94.0	—	−91.5	—	−90.5	—	89.8	—

a) 1 Å = 10 nm. b) Δ corresponds to the deviation from the isolated system (PM3).

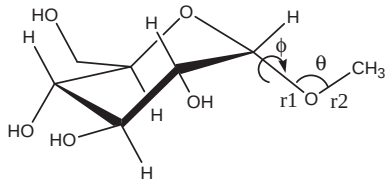

−7.8 to 1.2 degrees. It is noteworthy that the ONIOM method using the MM parameters, UFF, gave results similar to those obtained by the supermolecule method. The ONIOM(RHF/3-21G:PM3) and COSMO methods gave large Δ_{dihedral} values, approximately 30–60 degrees. In short, solvation greatly affected the dihedral angle of the methoxy group, which relates to the glycoside-bond part.

Figures 3a–3d show the orbital energies of frontier orbitals, HOMO and LUMO (the lowest unoccupied molecular orbital), of the solvated system of methyl derivatives of Glc′, Gal′, GalNAc′, NeuAc′, $(NeuAc)_2$, and NAD′, which were calculated by various methods: ONIOM(PM3:UFF), ONIOM(RHF/3-21G:PM3), PM3 with the supermolecule method, and PM3 with the COSMO method. The orbital energies of the isolated systems are shown in Figure 3e for comparison.

To determine the validity of using MM parameters for solvent as a "Low" level of theory, we focused on the energy profiles of HOMO based on the ONIOM(PM3:UFF) method and the more reliable Supermolecule(PM3) method. The profiles of the HOMO energies in Figures 3a-1 and 3c-1 were similar to each other. Especially, the HOMO energies of the monosaccharides by ONIOM (−10.8, −10.6, and −10.1 eV, respectively, for Glc′, Gal′, and GalNAc′) were very close to those by the supermolecule method (−11.2, −11.2, and −10.2 eV). The ONIOM values of NeuAc′, $(NeuAc)_2$, and NAD′ (−5.4, −3.0, and −5.7 eV) were similar to those by the supermolecule method (−8.0, −6.6, and −8.2 eV). Thus, the ONIOM method using MM parameters gave reasonable results for profiles of the orbital energies. The two types of ONIOM methods were also compared (Figures 3a-1 and 3b-1). When quantum methods were used instead of an UFF for ONIOM calculations, the HOMO energies changed slightly but maintained similar energy profiles, except for that of NAD′, which decreased from −5.7 to −8.4 eV. Interestingly, these observations regarding the orbital energies of frontier orbitals are also similar to those obtained in the isolated system (see Figure 3e-1).

Further, we selected a much larger basis set for the studied species so as to obtain better descriptions. Figures 3a-2, 3b-2, and 3c-2 show the orbital energies obtained by RHF single-point energy calculations with the 6-31++G(d,p) basis set as supermolecules at the optimized geometries by the ONIOM-(PM3:UFF), ONIOM(RHF/3-21G:PM3), and Supermolecule(PM3) methods, respectively. The three energy profiles were similar to one another, though using the larger basis set lowered the orbital energies of NeuAc′ and $(NeuAc)_2$, in all cases. Orbital energies were quite close to each other among Glc′, Gal′, and GalNAc′, and the relative energies were comparable among NeuAc′, $(NeuAc)_2$, and NAD′. The order of the orbital energies of HOMO was (Glc′ ≈ Gal′) < GalNAc′ < (NeuAc′ ≈ NAD′) < $(NeuAc)_2$.

In contrast, electronic features such as those mentioned above were not observed with the dielectric method model (COSMO), as shown in Figure 3d-1. There were only small differences among the orbital energies of HOMO for the monosaccharides. Since COSMO is a continuum dielectric model, solvent water molecules are not defined explicitly.

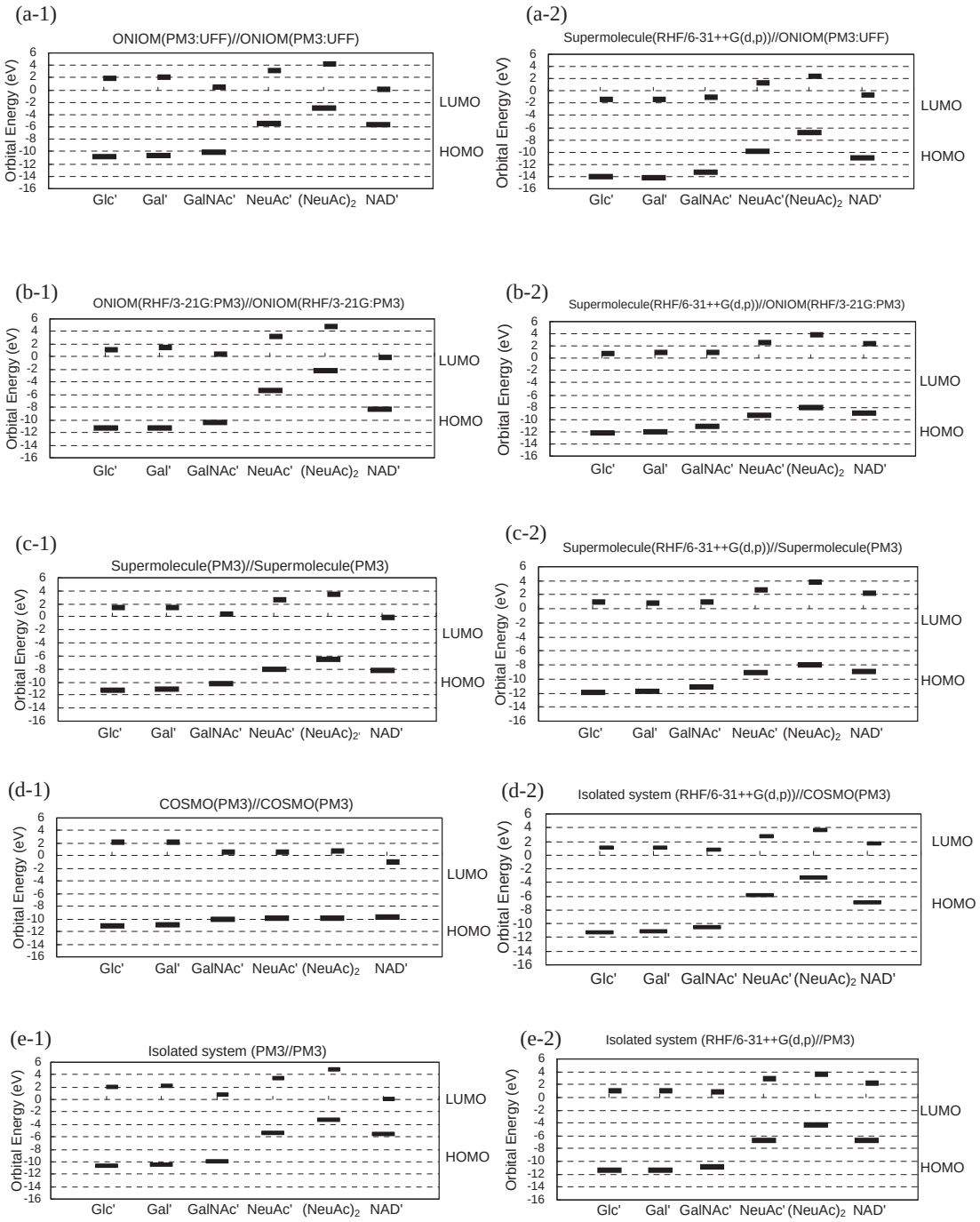

Figure 3. The orbital energies of frontier orbitals, HOMO and LUMO, of the studied monosaccharides as well as of dimeric sialic acid $(NeuAc)_2$ and NAD′. (a-1) in the hydration system calculated with ONIOM(PM3:UFF)//ONIOM(PM3:UFF), (a-2) in the hydration system calculated with the supermolecule method (RHF/6-31++G(d,p)) at ONIOM(PM3:UFF)-optimized geometries, (b-1) in the hydration system calculated with ONIOM(RHF/3-21G:PM3)//ONIOM(RHF/3-21G:PM3), (b-2) in the hydration system calculated with the supermolecule method (RHF/6-31++G(d,p)) at ONIOM(RHF/3-21G:PM3)-optimized geometries, (c-1) in the hydration system calculated with the supermolecule method (PM3//PM3), (c-2) in the hydration system calculated with the supermolecule method (RHF/6-31++G(d,p)) at PM3-optimized geometries, (d-1) in the hydration system calculated with COSMO(PM3)//COSMO(PM3), (d-2) as an isolated system using geometries optimized with the COSMO method (RHF/6-31++G(d,p)//COSMO(PM3), (e-1) as an isolated system (PM3//PM3), (e-2) as an isolated system (RHF/6-31++G(d,p)//PM3).

Therefore, the supermolecule method considering solvated molecules cannot be applied. Single-point energy calculations of the isolated solute system at the COSMO(PM3) optimized geometry were carried out. Energy levels of frontier orbitals for the isolated system at the RHF level of theory with the 6-31++G(d,p) basis set are shown in Figure 3d-2. Even

though geometric parameters, especially dihedral angles, were greatly changed by the COSMO method as mentioned above, the energy profiles were similar to those obtained by the other methods. The similarity between Figures 3d-2 and 3e-2 suggests that the geometric change for dihedral angle ϕ does not greatly affect the orbital energies. The changes in the dihedral angles in Table 2 and in the orbital energy profiles in Figure 3d-1 suggest that the COSMO method itself affects both the geometries and the orbital energies.

For comparison, the same larger basis set 6-31++G(d,p) was used for the isolated molecule (see Figure 3e-2). The obtained energy profile is similar to that of the isolated molecule shown in Figure 3e-1. The order of the HOMO energies was the same as that in the solvated system.

Orbital Energies of Gangliosides. RHF single-point energy calculations with a larger basis set 6-31++G(d,p) were applied to the hydrated system of a series of gangliosides and reference species such as NeuAc′, $(NeuAc)_2$, and NAD′. The ONIOM(PM3:UFF) and Supermolecule(PM3) geometries were adopted for the calculations. HOMOs of the solvated gangliosides were localized at the carboxyl groups, though they spreaded out slightly more than those of the unsolvated case reported in our previous paper. They were not extended to the glycoside linkages, of which the structures were affected by solvation. It is noteworthy that the feature of the localization of HOMOs are similar each other for the solvated and unsolvated models.

We paid special attention to the orbital energies of HOMO because of its nucleophilic behavior caused by the anionic sites in these molecules. As seen in Figure 4a at the ONIOM-(PM3:UFF) geometry, we found that the orbital energies of HOMO for G_{D2} (−8.4 eV) and G_{D3} (−8.1 eV) were higher than those for G_{M3} (−9.5 eV) and G_{M1b} (−10.4 eV). The orbital energy of HOMO of sialic acid (−9.8 eV) was close to that of NAD′ (−10.9 eV). The orbital energy of HOMO of dimeric sialic acid (−6.8 eV) was higher than that of any other species. The energy profile of the frontier orbitals of gangliosides in Figure 4a is quite similar to that in Figure 4b at the Supermolecule(PM3) geometry. In the latter case, the orbital energies of HOMO for G_{D2} (−8.1 eV) and G_{D3} (−8.4 eV) were higher than those for G_{M3} (−9.4 eV) and G_{M1b} (−9.6 eV). The orbital energies of HOMO of sialic acid NeuAc′ and NAD′ were almost the same as each other (−9.0 eV). Dimeric sialic acid $(NeuAc)_2$ had the highest value, −8.0 eV, among them, though that value was closer to those of G_{D2} and G_{D3} compared to the values calculated by Supermolecule(RHF/6-31++G(d,p)//ONIOM(PM3:UFF).

Figure 4c shows the orbital energies of frontier orbitals calculated with the RHF/6-31++G(d,p) method in the gas phase, as reported in our previous paper.[5] The profiles of orbital energies of HOMO in the gas phase were found to be quite similar to those calculated by the solvated models mentioned above.

Our previous work regarding the isolated system revealed that HOMO energies were correlated with the strength of the inhibitory effects of gangliosides. For example, the inhibitory effect of G_{D3} was larger than that of G_{M1b} (Figure 1a), which correlated well with the orbital energies of HOMO. Our findings with the solvation effect agree well with the previous

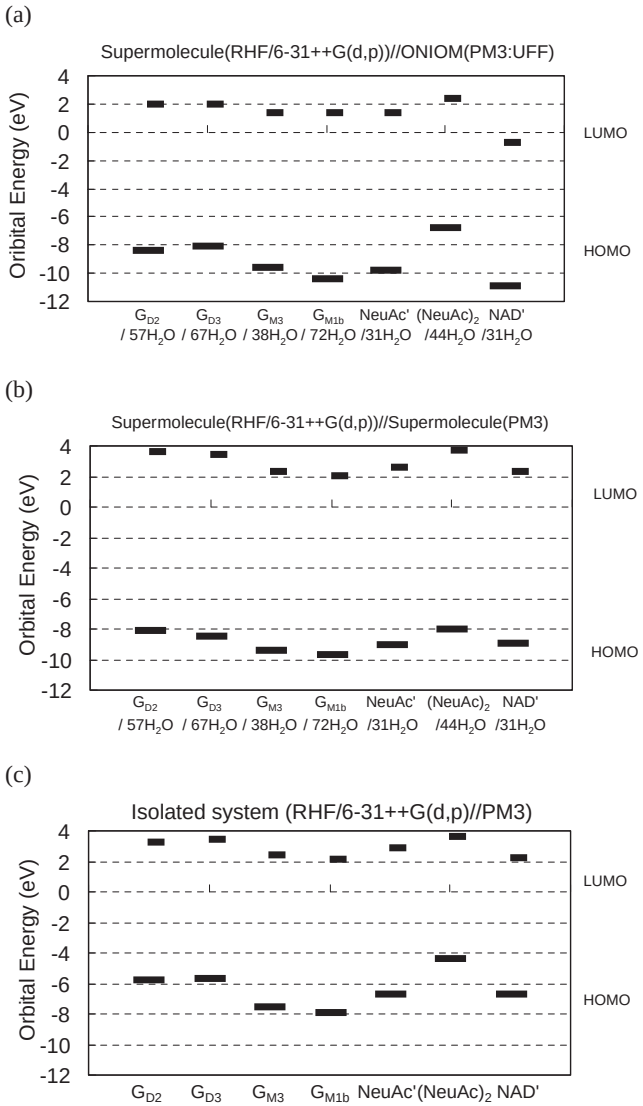

Figure 4. The orbital energies of frontier orbitals, HOMO and LUMO, of gangliosides as well as of sialic acid NeuAc′, dimeric sialic acid $(NeuAc)_2$, and NAD′. (a) Calculated as a supermolecule with the RHF/6-31++G(d,p)//ONIOM(PM3:UFF) method, (b) calculated as a supermolecule with the RHF/6-31++G(d,p)//PM3 method, (c) calculated as an isolated molecule with the RHF/6-31++G(d,p)//PM3 method.

study and indicate that the proposed mechanisms are appropriate even in the biological system.

Structural Changes of Sugar Part of Gangliosides by Solvation Effect. Structural change by the solvation effect on G_{D3} is shown in Figures 5 and 6 by superimposing the hydrated structures calculated with the ONIOM and supermolecule methods, respectively, on the isolated system. The structural change of the solute by solvation was small (Figures 5a and 6a). The change by the supermolecule method was only slightly larger than that with the ONIOM method according to their RMS values: 0.74 and 0.46, respectively. G_{D3} consists of a tandem sialic acid $(NeuAc)_2$, galactose (Gal), and glucose (Glc). In order to see which parts were affected by solvation,

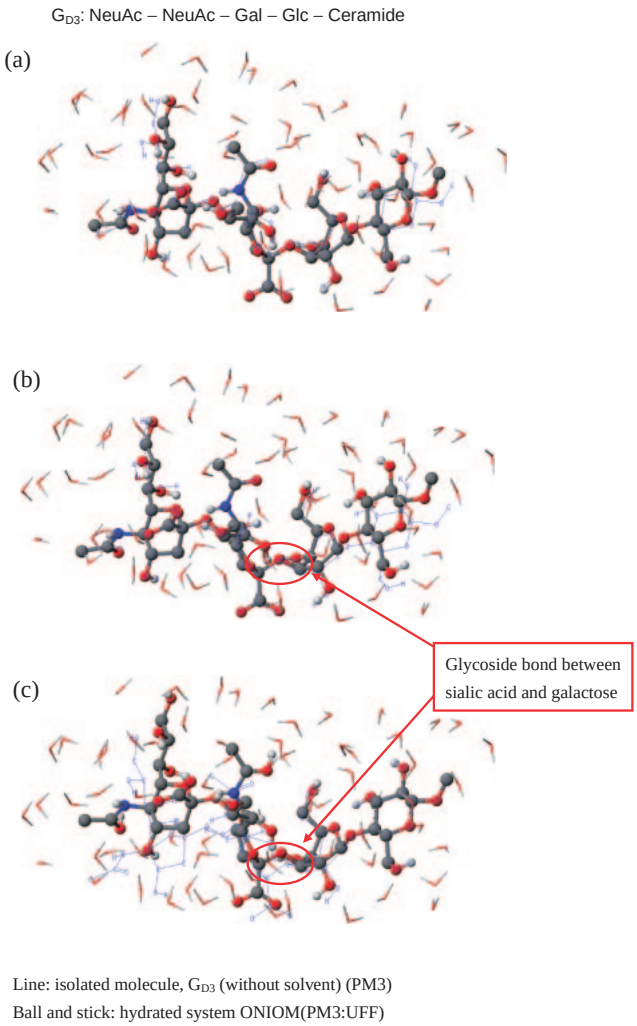

Figure 5. The structural change of the head group (sugar part) of G_{D3} by the solvation effect with the ONIOM-(PM3:UFF) method. (a) The structure optimized in the hydrated system calculated with ONIOM(PM3:UFF) (depicted by a ball-and-stick model) was superimposed with the structure optimized in the gas phase as an isolated molecule with the PM3 method (depicted by a line model). (b) The tandem sialic acid part on the left was partly superimposed. (c) The galactose–glucose on the right was partly superimposed.

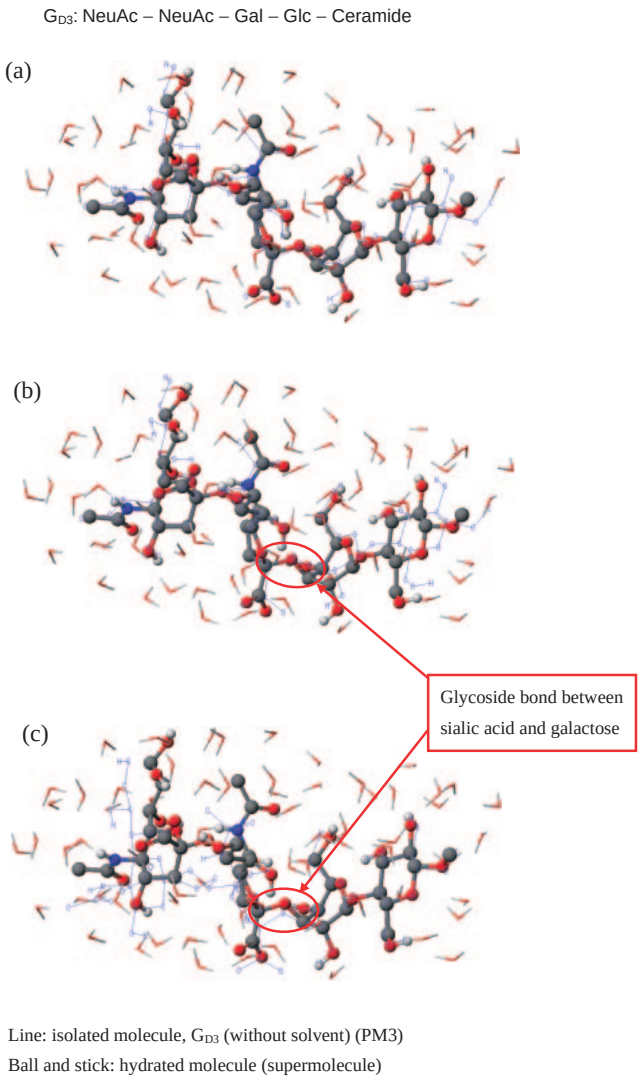

Figure 6. The structural change of the head group (sugar part) of G_{D3} by the solvation effect by considering the solvent and solute as a supermolecule. (a) The structure optimized as a supermolecule with the PM3 method (depicted by a ball-and-stick model) was superimposed with the optimized structure as an isolated molecule (depicted by a line model). (b) The tandem sialic acid part on the left was partly superimposed. (c) The galactose–glucose on the right was partly superimposed.

the tandem sialic acid part on the left was partly superimposed (Figures 5b and 6b), and the galactose–glucose (Gal–Glc) part on the right was partly superimposed (Figures 5c and 6c). One of the parts that solvation affected greatly was at the glycoside bond, a linkage part, between sialic acid and the galactose residue (see Figures 5b and 5c). This result partly relates to the ϕ value change by solvation listed in Table 2. In contrast, the structure of the tandem sialic acid residue itself, which is thought to be responsible for the inhibitory effect, did not change significantly by the solvation effect.

According to the recognition model by Yokoyama et al.,[2] the distance of the tandem sialic acid part from the membrane is one of the important factors. Table 3 tabulates selected distances between the membrane carbon and the carboxyl group, as well as those between two carboxyl groups of the tandem sialic acid in gangliosides (G_{D3}, G_{D2}, and G_{M3}). We defined the membrane carbon as the carbon in the methoxy group connected to C1 of glucose. The distances between the membrane carbons and the carboxyl groups of sialic acids, which were thought to be critical to the recognition by CD38,[2] are listed. The distances between two carboxyl groups (#3 and #4) of tandem sialic acid residues are also listed. The carboxyl groups of sialic acids in gangliosides are numbered according to the topological order of sialic acids in the sugar chain from the ceramide side; the carboxyl #3 group is closer to the membrane than the carboxyl #4 group (see Figure 1a). A comparison of the geometric parameters among the methods considering the solvent effect revealed that the ONIOM and supermo-

Table 3. Selected Distances between the Membrane Carbon and the Carboxyl Groups, and Those between Two Carboxyl Groups of the Tandem Sialic Acid in G_{D2}, G_{D3}, and G_{M3}

		Distance between the membrane carbon and the carboxyl group/Å[a),b)]		Distance between two carboxyl groups (#3 and #4)/Å[a),c)]		
		C(membrane) –C(carboxyl #3)	C(membrane) –C(carboxyl #4)	C(#3)–C(#4)	O1(#3)–O1(#4)	O2(#3)–O2(#4)
G_{D2}	ONIOM(PM3:UFF)	13.1	15.7	6.6	6.3	8.0
	Supermolecule(PM3)	13.1	16.0	6.5	6.5	7.6
	COSMO(PM3)	12.9	15.9	6.1	6.0	7.4
	Isolated system (PM3)	12.9	15.8	6.0	6.1	7.0
G_{D3}	ONIOM(PM3:UFF)	12.7	15.0	8.3	8.5	9.9
	Supermolecule(PM3)	12.1	14.2	7.9	8.2	9.7
	COSMO(PM3)	12.7	15.6	7.9	7.6	9.9
	Isolated system (PM3)	12.7	15.8	8.2	8.2	9.9
G_{M3}	ONIOM(PM3:UFF)	11.8				
	OINOM(HF/3-21G:PM3)	11.5				
	Supermolecule(PM3)	11.7				
	COSMO(PM3)	12.3				
	Isolated system (PM3)	12.1				

a) 1 Å = 10 nm. b) The carboxyl groups of sialic acids in gangliosides are numbered according to the topological order of sialic acids in the sugar chain from the ceramide side; that is, the carboxyl #3 group is closer to the membrane than the carboxyl #4 group. c) Distances between the two carboxyl groups (#3 and #4) of tandem sialic acid residues are listed.

Table 4. Energy Changes Due to the Structural Changes by Solvent Effect on the Head Group of Gangliosides: G_{D2}, G_{D3}, G_{M1b}, and G_{M3}

	G_{D2}	G_{D3}	G_{M1b}	G_{M3}
ΔE/kJ mol^{-1} a)	3.47	7.82	0.54	0.67

a) Structures of gangliosides used for this calculation were those optimized in the hydrated system by ONIOM(PM3:UFF) and those optimized as isolated molecules by the PM3 method.

lecule methods, except for the COSMO method, gave similar results. For example, the calculated values for the distance between the membrane and carboxyl group #3 of G_{M3} were 11.8 (ONIOM(PM3:UFF)), 11.5 (ONIOM(HF/3-21G:PM3)), 11.7 (Supermolecule(PM3)), and 12.3 Å (COSMO). There was only a slight difference between the obtained values in the hydrated system and those in the isolated system, e.g., 12.1 Å (PM3) for the isolated molecule and 11.5–11.8 Å (ONIOM and supermolecule methods) for the solvated system. In addition, the distances between the two carboxyl groups did not change significantly between the hydrated and isolated systems (0.2–1.0 Å). This geometric stability of the tandem sialic acids supports our findings that the tandem sialic acid residue plays a key role in the enzyme reaction as well as in the inhibitory effects on NAD glycohydrolase.

Table 4 lists the energy changes due to the structural changes by the solvent effect on the head group of gangliosides (G_{D2}, G_{D3}, G_{M1b}, and G_{M3}). The structures of gangliosides used for these calculations were those optimized in the hydrated system by the ONIOM(PM3:UFF) method and those optimized as isolated molecules by the PM3 method. The solvent effect on the energy change due to the geometry change was rather small (less than 8 kJ mol^{-1}).

Conclusion

In this paper, we report the electronic structures of gangliosides in the biological environment considering the solvation effect. Application of the ONIOM method to the gangliosides provided geometries and electronic structures similar to those obtained by the supermolecule method.

The superimposition of optimized structures revealed the effects of solvation on the structures of the tandem sialic acids, which showed only slight changes in the presence of solvent molecules. We found that the energies of HOMO correlated with the strength of the inhibitory effects in the solvation system; this correlation was also seen in the isolated systems. These results of careful study of the solvation effect indicate that our proposed model for the recognition mechanisms of NAD glycohydrolase is appropriate in the physiological environment. The modeling techniques with the supermolecule and ONIOM methods that we present in this paper will bring further understanding of other mechanisms involving large molecules in the biological system.

The authors thank the Research Center for Computational Science, Okazaki Research Facilities, National Institutes of Natural Sciences, Japan, for the use of the computer facilities. KN expresses her appreciation toward the financial support by Ajinomoto Scholarship Foundation.

References

1 M. Hara-Yokoyama, I. Kukimoto, H. Nishina, K. Kontani, Y. Hirabayashi, F. Irie, H. Sugiya, S. Furuyama, T. Katada, *J. Biol. Chem.* **1996**, *271*, 12951.

2 M. Hara-Yokoyama, Y. Nagatsuka, O. Katsumata, F. Irie, K. Kontani, S. Hoshino, T. Katada, Y. Ono, J. Fujita-Yoshigaki, H. Sugiya, S. Furuyama, Y. Hirabayashi, *Biochemistry* **2001**, *40*,

888.
3 M. Hara-Yokoyama, H. Ito, K. Ueno-Noto, K. Takano, H. Ishida, M. Kiso, *Bioorg. Med. Chem. Lett.* **2003**, *13*, 3441.
4 M. Hara-Yokoyama, *Curr. Med. Chem.* **2006**, *13*, 2233.
5 K. Ueno-Noto, M. Hara-Yokoyama, K. Takano, *J. Comput. Chem.* **2006**, *27*, 53.
6 M. L. Love, D. M. Szebenyi, I. A. Kriksunov, D. J. Thiel, C. Munshi, R. Graeff, H. C. Lee, Q. Hao, *Structure* **2004**, *12*, 477.
7 L. Onsager, *J. Am. Chem. Soc.* **1936**, *58*, 1486.
8 M. W. Wong, M. J. Frisch, K. B. Wiberg, *J. Am. Chem. Soc.* **1991**, *113*, 4776.
9 S. Miertus, E. Scrocco, J. Tomasi, *Chem. Phys.* **1981**, *55*, 117.
10 S. Miertus, J. Tomasi, *Chem. Phys.* **1982**, *65*, 239.
11 A. Klamt, G. Schüürmann, *J. Chem. Soc., Perkin Trans. 2* **1993**, 799.
12 J. B. Foresman, T. A. Keith, K. B. Wiberg, J. Snoonian, M. J. Frisch, *J. Phys. Chem.* **1996**, *100*, 16098.
13 R. Zhang, X. Ai, X. Zhang, Q. Zhang, *THEOCHEM* **2004**, *680*, 21.
14 N. U. Zhanpeisov, J. Leszczynski, *THEOCHEM* **1999**, *487*, 107.
15 F. Maseras, K. Morokuma, *J. Comput. Chem.* **1995**, *16*, 1170.
16 S. Dapprich, I. Komáromi, K. S. Byun, K. Morokuma, M. J. Frisch, *THEOCHEM* **1999**, *461–462*, 1.
17 M. Svensson, S. Humbel, R. D. J. Froese, T. Matsubara, S. Sieber, K. Morokuma, *J. Phys. Chem.* **1996**, *100*, 19357.
18 K. Kahn, T. C. Bruice, *J. Am. Chem. Soc.* **2000**, *122*, 46.
19 M. Torrent, T. Vreven, D. G. Musaev, K. Morokuma, O. Farkas, H. B. Schlegel, *J. Am. Chem. Soc.* **2002**, *124*, 192.
20 S. Re, K. Morokuma, *J. Phys. Chem. A* **2001**, *105*, 7185.
21 A. Pandey, S. N. Datta, *J. Phys. Chem. B* **2005**, *109*, 9066.
22 R. J. F. Branco, P. A. Fernandes, M. J. Ramos, *J. Phys. Chem. B* **2006**, *110*, 16754.
23 R. Zhang, X. Zhang, Z. Qu, X. Ai, X. Zhang, Q. Zhang, *THEOCHEM* **2003**, *624*, 169.
24 C. E. Kundrot, J. W. Ponder, F. M. Richards, *J. Comput. Chem.* **1991**, *12*, 402.
25 A. K. Rappe, C. J. Casewit, K. S. Colwell, W. A. Goddard, III, W. M. Skiff, *J. Am. Chem. Soc.* **1992**, *114*, 10024.
26 M. J. Frisch, G. W. Trucks, H. B. Schlegel, G. E. Scuseria, M. A. Robb, J. R. Cheeseman, J. A. Montgomery, Jr., T. Vreven, K. N. Kudin, J. C. Burant, J. M. Millam, S. S. Iyengar, J. Tomasi, V. Barone, B. Mennucci, M. Cossi, G. Scalmani, N. Rega, G. A. Petersson, H. Nakatsuji, M. Hada, M. Ehara, K. Toyota, R. Fukuda, J. Hasegawa, M. Ishida, T. Nakajima, Y. Honda, O. Kitao, H. Nakai, M. Klene, X. Li, J. E. Knox, H. P. Hratchian, J. B. Cross, V. Bakken, C. Adamo, J. Jaramillo, R. Gomperts, R. E. Stratmann, O. Yazyev, A. J. Austin, R. Cammi, C. Pomelli, J. W. Ochterski, P. Y. Ayala, K. Morokuma, G. A. Voth, P. Salvador, J. J. Dannenberg, V. G. Zakrzewski, S. Dapprich, A. D. Daniels, M. C. Strain, O. Farkas, D. K. Malick, A. D. Rabuck, K. Raghavachari, J. B. Foresman, J. V. Ortiz, Q. Cui, A. G. Baboul, S. Clifford, J. Cioslowski, B. B. Stefanov, G. Liu, A. Liashenko, P. Piskorz, I. Komaromi, R. L. Martin, D. J. Fox, T. Keith, M. A. Al-Laham, C. Y. Peng, A. Nanayakkara, M. Challacombe, P. M. W. Gill, B. Johnson, W. Chen, M. W. Wong, C. Gonzalez, J. A. Pople, *Gaussian 03, Revision D.02*, Gaussian, Inc., Wallingford CT, **2004**.